Segmentation of Agricultural Images using Vegetation Indices

Jean Fabrício Batista Santos, Jocival Dantas Dias Junior, André Ricardo Backes
and Maurício Cunha Escarpinati
School of Computer Science, Federal University of Uberlândia, Brazil

Keywords: Precision Agriculture, Plant Segmentation, Vegetation Indices.

Abstract: Identifying and segmenting plants from the background in agricultural images is of great importance for precision agriculture. It serves as a basis for several tasks such as identification of planting lines, identification of weed plants, agricultural automation, among others. Given this importance, in this paper, we evaluated the application of five vegetation indices for RGB images together with two binarization techniques for the plant/background segmentation process. The results showed promising performance in all evaluated indices. It was also possible to identify a relationship between the performance obtained in each index and the capture conditions in each dataset.

1 INTRODUCTION

The diversity of land areas, types of soils and plants, products, and machinery makes the management of a simple planting area a complex task. To facilitate this task, in the last few decades Precision Agriculture (PA) has emerged as a new way to manage agricultural resources. Literature defines PA as the use of different technologies (such as artificial intelligence, internet of things, data analysis, and image processing) with the main objective of optimizing results, reducing costs, and creating a more sustainable production chain.

A simple example of PA applied to a plantation is the use of an Unmanned Aerial Vehicle (UAV) to acquire images of the plantation. Depending on the sensors present in the UAV, it is possible to obtain a map of the area with many types of information, such as land topology and vegetation distribution. There is a wide range of sensors that can be used with a UAV. The most common are cameras that capture color patterns in RGB format. However, other bands, such as infrared and ultraviolet, can be also used. RGB cameras are widely used in image processing because they are the standard that most devices use, such as smartphones, allowing image processing algorithms to run even in mobile applications (Riehle et al., 2020). By using specific algorithms, it is possible to extract from these maps high-level information from the area, such as the location of crop lines, plant count, and the presence of sowing failures. These informations enable the farm to improve the use of the resources and allows the use of other operations such as robots, tractors, and autonomous pruning (Bargoti and Underwood, 2016).

Identifying and separating plants from the soil is an important task because it allows the monitoring of plant growth, health, and the identification of pests and weeds. Mathematical equations applied to the RGB channels of the images result in different indices that highlight certain wavelengths, such as the green levels of the image, thus facilitating the separation of the plant from background pixels (Riehle et al., 2020). However, an index that highlights green pixels is not enough to separate weed crops, and other types of vegetation index may be needed for this problem. The use of vegetation indices has some advantages such as low computational cost in comparison with other segmentation techniques or machine learning approaches, easy implementation, and handling. Nevertheless, they are sensitive to brightness variation, presence of shadows, and manual definition of the threshold (Riehle et al., 2020).

In literature, there are a wide variety of RGB indices that can be used for image segmentation purposes. In the present work, we aimed to evaluate some of these vegetation indices in a plant/soil segmentation task when combined with a clustering algorithm and a simple threshold method to obtain the different regions of interest. We compared the performance of each vegetation index in the dataset presented in (Riehle et al., 2020), which presents images with predefined masks of the plant/soil regions.

The remaining of the paper is structured as fol-

Santos, J., Dias Junior, J., Backes, A. and Escarpinati, M.
Segmentation of Agricultural Images using Vegetation Indices.
DOI: 10.5220/0010325005060511
In *Proceedings of the 16th International Joint Conference on Computer Vision, Imaging and Computer Graphics Theory and Applications (VISIGRAPP 2021) - Volume 4: VISAPP*, pages 506-511
ISBN: 978-989-758-488-6

lows: Section 2 presents a review of recent paper published on this topic and that motivated our research. In Section 3 we describe the vegetation indices used in this work as also the datasets used for evaluation. Section 4 describes how experiments were performed while Section 5 presents the results obtained by each vegetation index. Finally, Section 6 concludes the paper.

2 RELATED WORK

Computing a vegetation index is a common preprocessing technique used for plant/soil segmentation problems. It increases the contrast between vegetation and soil, generating a grayscale image that highlights particular regions of interest. For example, the Excess Green Index (ExG) and the Excess Red Index (ExR) aim to increase the contract of the Green and Red levels, respectively, highlighting the plant from other elements, such as soil and waste. And when combined, these indices can generate even more efficient results in segmentation, such as ExGR (Riehle et al., 2020), which is calculated as follows:

$$ExG = 2G - R - B \tag{1}$$

$$ExR = 1.4R - B \tag{2}$$

$$ExGR = ExG - ExR \tag{3}$$

ExGR index results in an image where pixels range from positive (plant) to negative (soil and residues) values so that the image is easily segmented using a fixed threshold at zero value, without the need to use an automatic threshold method, such as Otsu (Otsu, 1979).

Another way to use these indices is to generate masks from the indexed image. While the ExG index highlights the pixels of the green channel of the image, the ExR index highlights the red channel. These two indices can be used to produce a mask for, respectively, vegetation and background, that combined by a logical AND operation enable us to extract the vegetation of the original image (Riehle et al., 2020).

Other methods can be used to segment plant/background without the need for manual parameterization (e.g., threshold or color selection). Some approaches use Naive Bayes to classify the pixels belonging to the plant and background (Abbasi and Fahlgren, 2016). First, the image is converted from RGB to HSV color model. Then, the color distribution of vegetation and soil are approximated by probability distribution functions, which allows the use of the Naive Bayes method to segment the plants.

More recently, deep learning approaches, such as Deep Convolutional Neural Networks (DCNN's), have been proposed as an alternative for plant/soil segmentation problems. This is explained due to their great success in many classification and segmentation problems in different areas. They have been proven to be very efficient in identifying objects and as a generic solution for various types of soils, terrains, and exposure to sunlight and shading. The network architecture varies from problem to problem as, for example, the number of convolutional and pooling layers (Zhuang et al., 2018). Depending on the application, the input can be images generated from the vegetation indices or simple RGB images. Performance analysis, however, shows that vegetation indices generate information loss and that using RGB images as input usually generates better results (Zhuang et al., 2018). For segmentation purposes, the basic structure of a DCNN is composed of an encoder and a decoder. The encoder is trained to compress and to extract image features by using several convolutional layers, organized hierarchically, where each layer corresponds to a different semantic level. In the sequence, the decoder reconstructs the input image based on the model compressed by the encoder, thus resulting in an image labeled with different regions of interest.

3 MATERIALS AND METHODS

3.1 Vegetation Indices

Given its usage in several precision agriculture works, we evaluated the following plant/background indices for segmentation: Modified Green Red Vegetation (4) (Bendig et al., 2015), Green Leaf Index (Equation 5) (Louhaichi et al., 2001), Modified Photochemical Reflectance Index (Equation 6) (Yang et al., 2018), Red Green Blue Vegetation Index (Equation 7) (Bendig et al., 2015), Excess of Green (Equation 8) (Woebbecke et al., 1995) and Vegetativen (Equation 9) (Hague et al., 2006):

$$MGRV = \frac{G^2 - R^2}{G^2 + R^2} \tag{4}$$

$$GLI = \frac{2G - R - B}{2G + R + B} \tag{5}$$

$$MPRI = \frac{G - R}{G + R} \tag{6}$$

$$RGBVI = \frac{G - (B * R)}{(G^2) + (B * R)} \tag{7}$$

$$ExG = 2G - R - B \quad (8)$$

$$VEG = \frac{G}{R^a * B^b} \quad (9)$$

* a = 0.667 and b = (1-a)

While ExG, GLI and VEG highlight pixels in the green channel, MGRVI, MPRI, and RGBVI highlight more than one channel of the image. For example, MGRVI enhances the information of both green and red channels, while MPRI emphasizes the reflectance produced by chlorophyll present in leaves. These indices act directly with the ability of the soil and plants to reflect, respectively, red and green shades. Figure 1 shows an example of the MGRVI index obtained for an image.

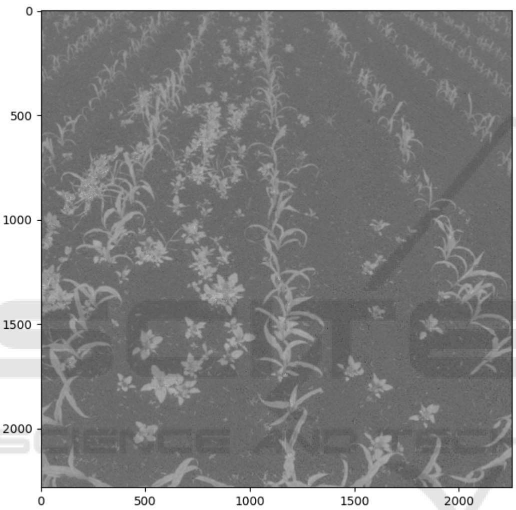

Figure 1: Example of the MGRVI index obtained for an image.

3.2 Dataset

To evaluate the proposed method we considered four datasets presented in (Riehle et al., 2020). Each dataset contains 50 images and it was obtained using a different camera, resulting in a total of 200 images. The cameras used for the first two sets were "GoPro HERO6 BLACK" and "Parrot SEQUOIA +" which originated the datasets, respectively, GP and SE. These images were obtained by an autonomous caterpillar robot "Phoenix". The other data set called K2 was obtained by the robot "TALOS" using a "Microsoft Kinect v2" camera and the fourth dataset was made available by the University of Bonn using a "JAI AD-130GE" camera. For all camera datasets images have 2280×2256 pixels size in RGB format. The datasets contain images of different plants (maize and sugar beet) at various growth stages and vegetation coverages.

3.3 Evaluation

We used five metrics to assess the performance of the proposed segmentation approach: Dice coefficient (Equation 10), Jaccard index (Equation 11), Precision (Equation 12), Sensitivity (Equation 13) and Specificity (Equation 14). In these equation, A and B are, respectively, the proposed and the expert's segmentation images, TP is the number of true positives, FN is the false negative and TN is the true negative.

$$Dice = \frac{2|A \cap B|}{|A| + |B|} \quad (10)$$

$$Jaccard = \frac{|A \cap B|}{|A \cup B|} \quad (11)$$

$$Precision = \frac{TP}{TP + FN} \quad (12)$$

$$Sensitivity = \frac{TP}{TP + FN} \quad (13)$$

$$Specificity = \frac{TN}{TN + FP} \quad (14)$$

4 EXPERIMENTS

In our experiments, we aimed to segment images in each dataset in order to extract the regions containing plants from the background image. To accomplish that we computed all selected vegetation indices for each image in the datasets. In the sequence, we used the K-means method to group the pixels into two classes ($K = 2$), i.e., Plant and Background. We initialized the centroids with the highest and lowest value present in the image for each index. This was performed to avoid any randomness and to guarantee the reproducibility of the algorithm. By associating the clusters obtained from K-means with the original pixel position, we obtain a binary image representing the two clusters, i.e., a segmented image representing regions of plant and background. Additionally, we used an opening morphological operation, with a 15×15 structuring element in square format, to remove small noises in the segmented image.

The selected 15×15 kernel size of the structuring element was defined manually and gradually. We started with a 5×5 kernel size and we increased its size as it kept reducing the presence of small noises and improved the result. The decision to use a square kernel was not based on any particular need, but due to the fact this kernel is commonly used in morphological opening and closing operations.

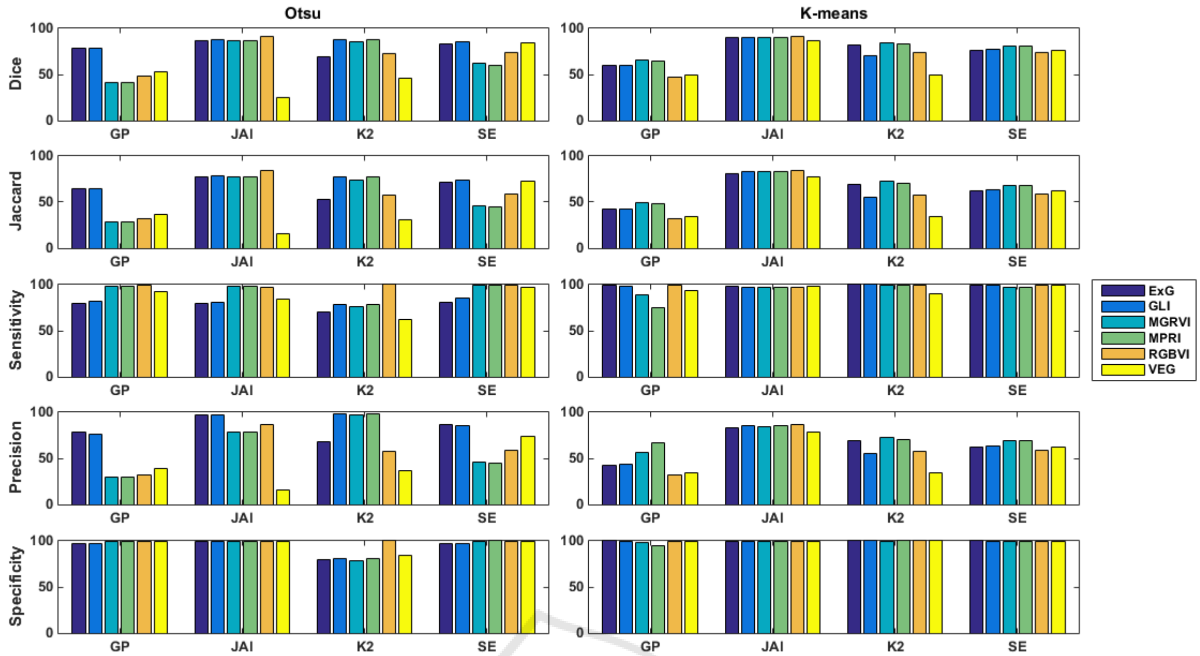

Figure 2: Comparison results for Otsu and K-means method for each vegetation index in all datasets.

Alternatively, we also evaluated the performance of a simple automatic threshold approach to segment the vegetation index images. In this case, we replaced the K-means method in the approach previously described by the Otsu method.

5 RESULTS

In this section, the results obtained by the experiments conducted on this work were presented. Each vegetation index was applied to each dataset as explained in Section 3. Figure 2 shows the results obtained in each metric by each vegetation index in all datasets, for both K-means and the Otsu method.

In general, the best results are obtained in the JAI dataset. Images in this dataset present small variation in luminosity and brightness, increasing the effectiveness of segmentation, which is corroborated by Dice coefficients ranging from between 86.82% to 91.31%. We also notice that, for this dataset, the K-means approach is slightly superior in comparison to Otsu. Moreover, this dataset presents a small variation in green shades present in the plants and the soil color pattern is very homogeneous (Figure 3). On the other hand, the GP dataset presented, in general, the worst results. This is explained due to the large variation of luminosity present in the images, as shown in Figure 4. A superficial analysis of the images in this dataset shows there exists a variation in luminosity caused by the local climate, as also an increase in the

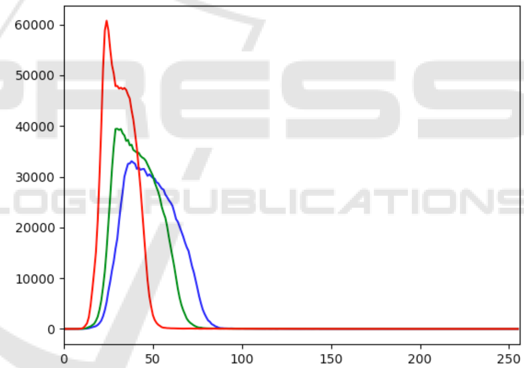

Figure 3: Example of histogram of an image from JAI dataset.

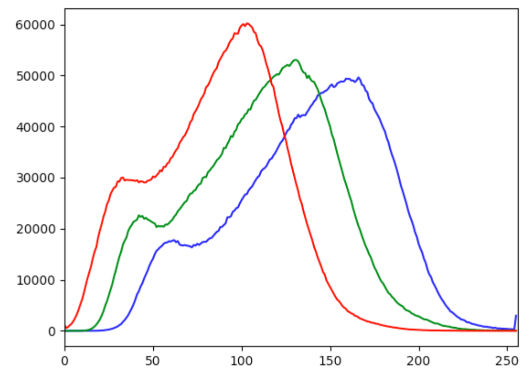

Figure 4: Example of histogram of an image from GP dataset.

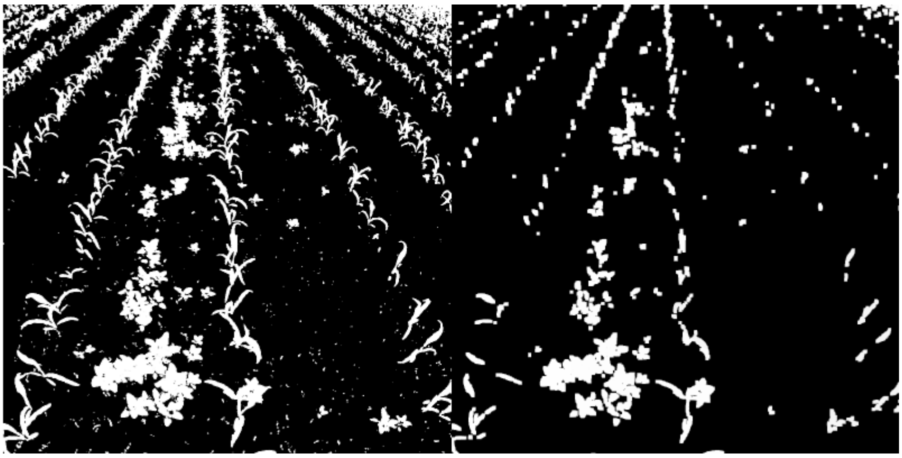

Figure 5: Noise reduction using morphological opening over the result of the K-means approach. Left: Binary image obtained from segmentation. Right: Image after morphological opening.

image exposure due to differences in the reflection of the sunlight by the soil. Even for images where there was small light variation, as in the SE dataset, the difference in the reflection of light on the ground still influences the results.

When comparing Otsu and K-means, we notice that K-means tend to obtain higher results. For the same dataset, Otsu presents higher oscillation in their results depending on the vegetation index used. Meanwhile, K-means, on average, presents similar results for different vegetation indices. This indicates that the process of clustering can detect more efficiently different regions of interest (soil and plant) than thresholding. This is partially explained by the fact that K-means uses a distance metric to compute the clusters and iteratively moves the centroid for the positions that best separate the different classes of objects.

We must also emphasize the importance of morphological opening, as shown in Figure 5. As one can notice, this operation diminishes the level of noise (e.g., loose pixels and other small objects) resulting from the segmentation process.

Among all compared indices, MGRVI presented the best results for the Dice coefficient, ranging from 65.0% to 90.0%. This is a normalization of GRVI whose vegetation and soil reflectance pattern is relatively easy to interpret, where the vegetation reflects the green band more than the red, while the soil reflects the red band more than the green (Motohka et al., 2010). Figure 6 shows the best segmentation obtained using K-means for each dataset.

6 CONCLUSIONS

In this paper, we presented a study of different vegetation indices to segment plants/soil in images. We evaluated two approaches to segment the images from four different datasets: K-means and Otsu. Results demonstrated the superiority of the K-means method to segment these images when applied in combination with the MGRVI index. The evaluation carried out by this work gives us an overview of the behavior of each vegetation index for different types of images (acquired at different conditions and equipment) and their limitations, making it clear that a single index may not be satisfactory to segment plants from the background. In future work, we intend to combine different vegetation indices to obtain a more robust result for different datasets, to evaluate whether the use of other color model (e.g., HSV) combined with vegetation indices can improve the result obtained, and evaluate different automatic threshold methods. We also intend to study the application of vegetation indices that use multispectral images for the plant/background segmentation process.

ACKNOWLEDGEMENTS

André R. Backes gratefully acknowledges the financial support of CNPq (Grant #301715/2018-1). This study was financed in part by the Coordenação de Aperfeiçoamento de Pessoal de Nível Superior - Brazil (CAPES) - Finance Code 001.

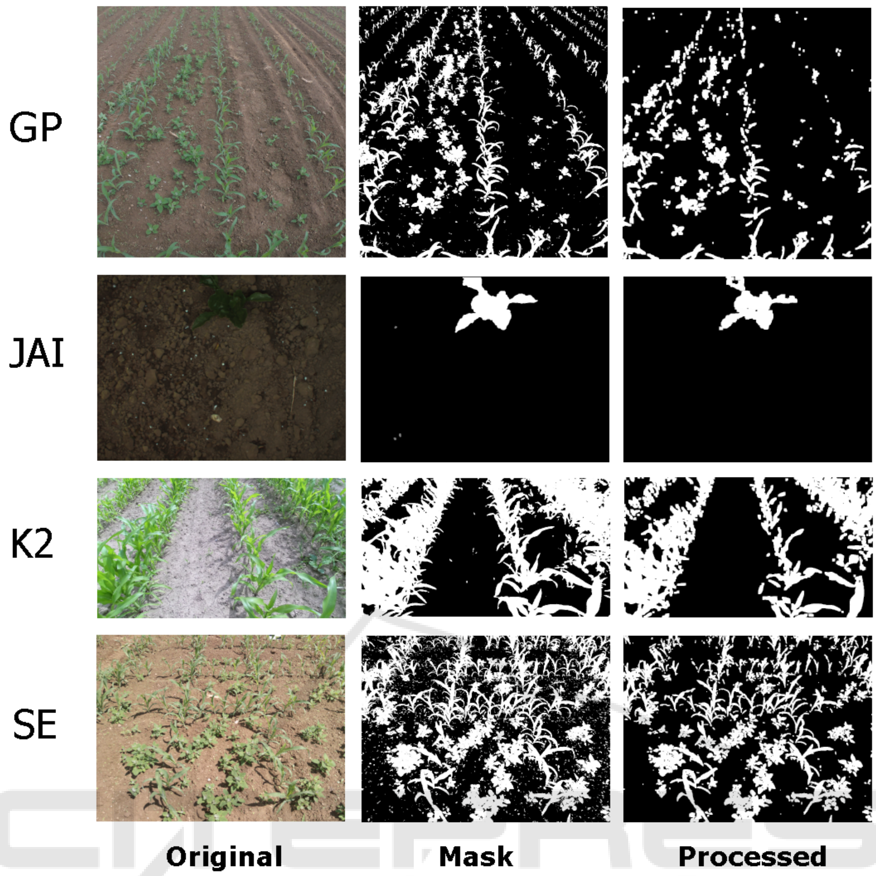

Figure 6: Best results obtained for each dataset. For datasets GP and K2, best results is obtained using MGRVI index. For JAI dataset, best result is obtained using RGBVI, while MPRI index performs best in SE dataset.

REFERENCES

Abbasi, A. and Fahlgren, N. (2016). Naïve bayes pixel-level plant segmentation. In *2016 IEEE Western New York Image and Signal Processing Workshop (WNYISPW)*, pages 1–4.

Bargoti, S. and Underwood, J. P. (2016). Image segmentation for fruit detection and yield estimation in apple orchards. *CoRR*, abs/1610.08120.

Bendig, J., Yu, K., Aasen, H., Bolten, A., Bennertz, S., Broscheit, J., Gnyp, M. L., and Bareth, G. (2015). Combining uav-based plant height from crop surface models, visible, and near infrared vegetation indices for biomass monitoring in barley. *International Journal of Applied Earth Observation and Geoinformation*, 39:79 – 87.

Hague, T., Tillett, N., and Wheeler, H. (2006). Automated crop and weed monitoring in widely spaced cereals. *Precision Agriculture*, 7:21–32.

Louhaichi, M., Borman, M., and Johnson, D. (2001). Spatially located platform and aerial photography for documentation of grazing impacts on wheat. *Geocarto International*, 16.

Motohka, T., Nasahara, K., Hiroyuki, O., and Satoshi, T. (2010). Applicability of green-red vegetation index for remote sensing of vegetation phenology. *Remote Sensing*, 2.

Otsu, N. (1979). A threshold selection method from gray-level histograms. *IEEE Transactions on Systems, Man, and Cybernetics*, 9(1):62–66.

Riehle, D., Reiser, D., and Griepentrog, H. W. (2020). Robust index-based semantic plant/background segmentation for rgb- images. *Comput. Electron. Agric*, 169:105201.

Woebbecke, D., Meyer, G., Bargen, K., and Mortensen, D. (1995). Color indices for weed identification under various soil, residue, and lighting conditions. *Transactions of the ASAE*, 38:259–269.

Yang, S., Wang, L., Shi, C., and Lu, Y. (2018). Evaluating the relationship between the photochemical reflectance index and light use efficiency in a mangrove forest with spartina alterniflora invasion. *International Journal of Applied Earth Observation and Geoinformation*, 73:778 – 785.

Zhuang, S., Wang, P., and Jiang, B. (2018). Segmentation of green vegetation in the field using deep neural networks*. In *2018 13th World Congress on Intelligent Control and Automation (WCICA)*, pages 509–514.